Asian Journal of Atmospheric Environment
Vol. 2-1, pp.26-33, June 2008

Physicochemical Properties of Asian Dust Sources

Chang-Jin Ma*, Mikio Kasahara[1], Susumu Tohno[2] and Ki-Hyun Kim[3]

Department of Environmental Science, Fukuoka Women's University, Fukuoka, Japan
[1]Institute of Science and Technology Research, Chubu University, Aichi, Japan
[2]Graduate School of Energy Science, Kyoto University, Kyoto, Japan
[3]Department of Earth and Environmental Sciences, Sejong University, Seoul, Korea

*Corresponding author. Tel: +81-92-661-2411, E-mail: ma@fwu.ac.jp

ABSTRACT

In order to fully understand the chemical properties of Asian dust particles, especially their transformation and aging processes, it is desirable to investigate the nature of original sands collected at local source areas in China. This study presents the detailed properties of sands collected at four different desert regions (Yinchuan, Wuwei, Dulan, and Yanchi) in China. Most of sands have irregular shape with yellowish coloration, whereas some of them show peculiar colors. The relative size distribution of sands collected at Yinchuan, Wuwei, and Dulan deserts exhibits monomodal with the maximum level between 200 and 300 μm, whereas that of Yanchi desert is formed between 100 and 200 μm. The mass concentration ratio of each element to that of Si (Z/Si) determined by PIXE analysis has a tendency towards higher Z/Si ratios for soil derived elements. It was possible to visually reconstruct the elemental maps on the surface of individual sands by XRF microprobe technique. In addition, the multielemental mass concentration could be quantitatively calculated for numerous spots of desert sands.

Key words: Asian dust, Desert sand, X-ray fluorescence, Long-range transport, Element

1. INTRODUCTION

In springtime, the weather in Asia produces intense dust storm originating from the Gobi Desert along the northern China/Mongolia border and other parts of desert China. This dust storm is a well-known springtime meteorological phenomenon throughout the East Asia as well as the Pacific Ocean.

Numerous studies on the Asian dust particles have been performed and reported (Song *et al.*, 2006; Lafon *et al.*, 2004; Ma *et al.*, 2004a; Song and Carmichael, 1999; Zhang *et al.*, 1998; Iwasaka *et al.*, 1988; Braaten *et al.*, 1986; Darzi *et al.*, 1982; Duce *et al.*, 1980). It is presumed that the chemistry of Asian dust particles can be influenced by absorption of atmospheric gases and subsequent oxidation of the absorbed gases on the surface during long-range transport. It is however desirable to explain how man-made pollutants and sea-salt aerosol react with natural Asian dust storm particles. In order to understand these denaturations of Asian dust particles, information of the nature of original sands at the local source areas is prerequisite. However, unfortunately, relatively little is known about the individual dust sands in various source regions (Nishikawa *et al.*, 2000).

The primary goal of this study is to report the comparative characteristics of bulk sands collected at four different desert regions in China. In addition, the chemical composition and the visual distribution on individual sands were newly determined.

2. EXPERIMENTAL METHODS

2. 1 Description of Sampling Sites

Dust storm is found at high frequency (with more than 30 days) in the Taklimakan desert on yearly basis. Likewise, yearly dust storms of more than 15-20 days is situated in the Gobi Deserts in the west of the upper Yellow River valley, the middle Yellow River valley, and northern North China (Qian *et al.*, 2004)

The sedimentation of the whole gigantic particles (e.g., larger than 10 μm) happens near the source region of dust storm (Husar *et al.*, 2001). It is a generally acknowledged fact that Taklimakan desert, which is a long way off from receptor areas, does not exert much impacts on receptor areas. In light of this, four desert areas (Yinchuan, Wuwei, Dulan, and Yanchi) located nearby Gobi desert were chosen in the present study (see Fig. 1).

Yinchuan lies in the middle of the Yinchuan or Ningxia Plain. It is sheltered from the deserts of Mongolia by the high ranges of the Helan Mountain on its west. The Yellow River runs through Yinchuan

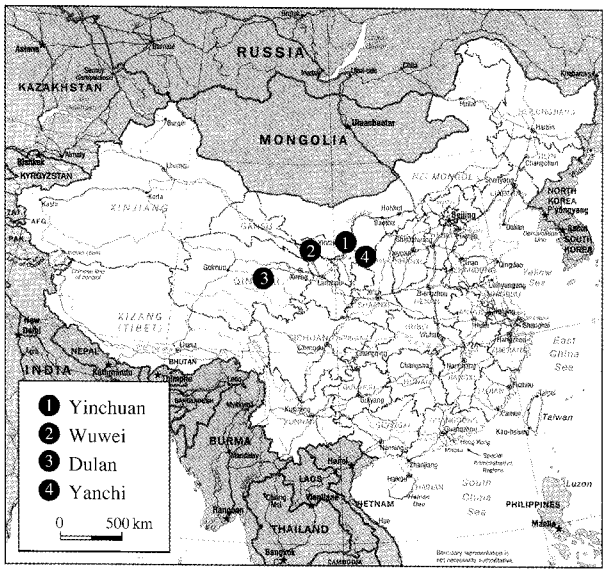

Fig. 1. Map showing the desert areas of sand collection.

from southwest to northeast. Yinchuan has a temperate continental climate with an annual average temperature of 8.5°C, with 158 frost-free days. Its annual rainfall averages 200 millimeters.

Traditionally, Yinchuan was an administrative and commercial center. In recent year, extensive coal deposits discovered on the eastern bank of the Yellow River, near Shizuishan, 100 km to the north, have made Shizuishan a coal-mining center (China Development Brief).

Wuwei is situated in the central part of Gansu province, on the east end of Hexi Corridor. It is located at the juncture of Qinghai-Tibetan plateau, Loess plateau and Mongalian-Xinjiang plateau. Wuwei has a temperate semiarid climate with an annual average temperature of 8.7°C, with frost free period of 165 days and annual precipitation of 158 mm (China Development Brief).

Dulan County belongs to West Lake Mongolia & Tibetan Autonomous prefecture, Qinghai Province. It is located at the southeast of Chaidamu Basin, 467 kilometers away from southwest of Xining. One part of the road from Dulan to Geermu is at the heart of the vast desert of Chaidamu Basin. It was also an important stop of the famed Silk Route.

Dulan is cold and semiarid. The mean annual temperature is 3°C with a January average of −10°C and a July average of 15°C, and the mean annual precipitation is 188 mm, 78% of which falls from May through September (China Development Brief).

Yanchi lies in the semi-deserts of the arid north west. Consecutive years of drought have left the county parched and barren. Due to increasing problems of desertification, Yanchi has frequently adopted with new grazing practices, sometimes based on principles of traditional Mongol range management. It is of typical temperate zone of continental monsoon climate. There is less rain but more wind all the year round, and weather is extremely dry. The mean annual temperature is 9.2°C (−7°C (January) to 20.4°C (July)) with mean annual precipitation of 225 mm (China Development Brief).

2.2 Sampling of Desert Sands

If a sand sample is representative enough, it can give an average estimate of the whole area desert. In fact, the importance of a representative soil sample is readily apparent prior to laboratory preparation, extraction, analysis and interpretation of results. To obtain a representative sand sample, three different points (within a 500 m radius) were selected separately and randomly for each desert. A spade which is one of common tools used to sample soil was applied to collection of surface sands. A 15 cm long tube with a diameter of 22 mm was chosen as the storage container. They are made of scratch-free Pyrex. Each tube was fully filled with compacted sand. After sealing with Teflon tape and wrapping with aluminum foil, every sand sample was placed in a cold storage bag during air transportation. All tubes were refrigerated until analysis.

2.3 Chemical Identification

The same amounts (2 g of dried sands) of desert sands collected among three different points were evenly mixed. The mixed desert sands were dissolved in 20 mL of pure deionized water and mixed in an ultra-sonicator for 20 min. After ultrasonic extraction, the sample was allowed to be filtered through the Nuclepore® filter with a 0.2 μm pore size. To completely separate the water-soluble fractions from the insoluble solids, the filtrate was then centrifuged at 4,000 rpm (maximum centrifugal force: 2,670 g) for 20 min.

To determine the elemental concentration, both soluble and insoluble fractions of sands were submitted for Particle Induced X-ray Emission (PIXE) installed in Quantum Science and Engineering Center, Kyoto University. Since the self-absorption of emitted characteristic X-ray can occur when specimens are thick, the insoluble solid sands were pulverized and homogenously deposited onto a polycarbonate substrate film. Then they were irradiated by the proton beam of PIXE system. Due to analytical difficulties with the liquid samples by PIXE, a 20 μL water soluble fraction was mounted on a polycarbonate substrate film and dried under infrared lamp.

PIXE analysis was performed with a proton beam of 6 mm diameter and 2.0 MeV energy from a Tandem Cockcroft. Beam intensities of 10 to 60 nA were employed with the total dose of about 20 μC. X-ray with the energy of 14.8 keV emitted from the target was detected by a Si (Li) detector which had a resolution of 152 eV at 5.9 keV. The more detailed analytical procedures and experimental set-up used for PIXE analysis have been described elsewhere (Ma *et al.*, 2001).

To analyze the chemical structure and mixing state of surface and inner individual sands, X-ray fluorescence (XRF) microprobe system equipped at SPring-8 BL37XU was applied. Hayakawa (2000) established this BL-37XU at SPring-8 that allows chemical analysis for a wide variety of specimens. This method has been successfully used to carry out the reconstruction of elemental map with the quantification of multiple elements at femto gram level sensitivity (Hayakawa *et al.*, 2001). A combination of the focusing mirror and a fixed exit monochromator has enabled energy tunable X-ray microbeam. The samples were placed on the XY stage in a vacuum chamber, and the takeoff angle of 10° was used for the measurement. The intensity of the incident X-rays was monitored by an ionization chamber. The fluorescence X-rays were recorded with a Si (Li) detector placed in the electron orbit plane of the storage ring and mounted at 90° to the incident X-rays to minimize background caused by the scattering. More details about the analytical procedures and experimental set-up for XRF microprobe analysis can be found in Hayakawa *et al.* (2001).

3. RESULTS AND DISCUSSION

3.1 Physical Properties

3.1.1 Morphology and Color

The morphology of original desert sands collected from four different desert areas was displayed in Photo 1. Nearly all of sands have irregular shape with yellowish coloration, whereas some sands show peculiar colors such as bluish, blackish, and reddish. Minerals are colored because certain wavelengths of light are absorbed. It is suggested that this color dissimilarity is influenced largely by chemical composition and atomic structure of the mineral. Idiochromatic color in mineral can be caused by the presence of elements like Cu and Mn in the mineral. For example, Cu in azurite, Cu in malachite, and Mn in rhodonite show blue, green, and pink color, respectively (Bates and Jackson, 1987). Chromaphore color can be caused by the presence of a small concentration of elements like Fe, Mn, Cu, Cr, Co, Ni, and V. Green quartz, black calcite, and red color in many minerals can be caused by dispersions of chlorite, MnO_2, and hematite, respectively (Bates and Jackson, 1987).

3.1.2 Size Distribution

Fig. 2 illustrates the size distribution of original sands collected at four desert areas in China. The size of individual sands was calculated with the mean of apse line and minor line of each sand by using digital

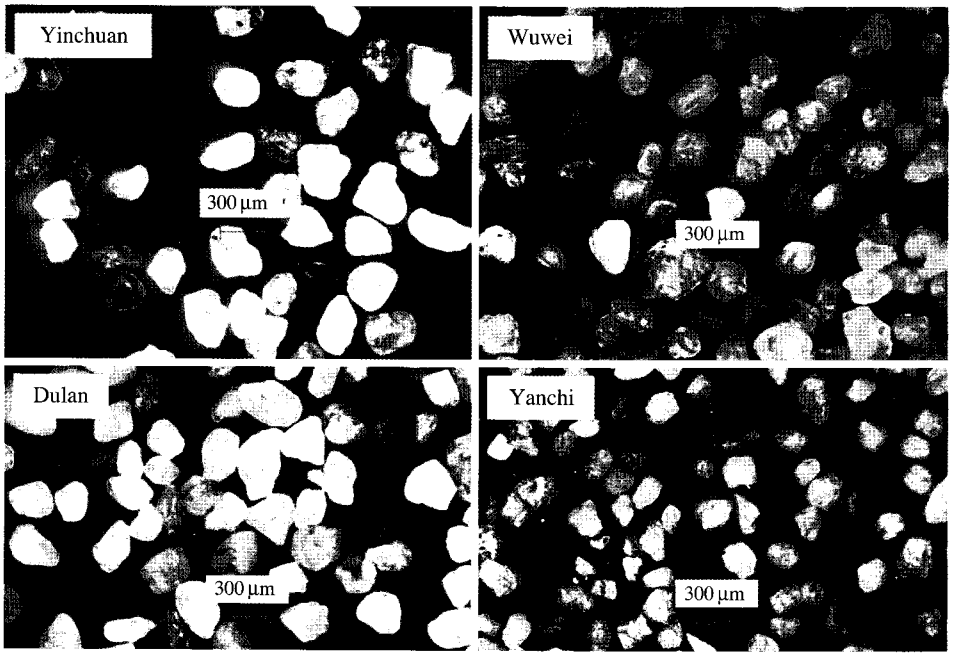

Photo 1. Microscopic image of sands collected at four desert areas in China (× 100).

microscope (KEYENCE, VH-7000). For each sample, 500 sands were selected randomly for their sizing. The shape of size distribution for sands collected at Yinchuan, Wuwei, and Dulan sites is monomodal to show the maximum level between 200 and 300 μm. On the other hand, the maximum level for Yanchi desert sands is displayed between 100 μm and 200 μm. The size of sands at Wuwei desert area is relatively wide spread in the range up to 600 μm. As shown in Photo 1, the size of original sands collected at Yanchi desert site is relatively smaller than those collected at other three sites. In addition, many broken pieces of sand at several micrometer size are observed in the field of Yanchi sands. Hence, the sands of Yanchi desert area are to be fragmented into tiny pieces by aeolian processes. This desert dust finally dissipates when the dust particles are removed from the atmosphere by dry and/or wet removal processes (Ma *et al.*, 2004b). As mentioned earlier, gravitational settling of desert sands and large dust particles (>10 μm) occurs near the desert regions within the first day of transport (Husar *et al.*, 2001).

Wet removal occurs sporadically throughout the 5-10 day lifetime of dust particles with the remaining smaller size (Husar *et al.*, 2001). Desert dust interaction with clouds results in cloud scavenging, while clouds can be removed by precipitation (Desboeufs *et al.*, 2001). Cloud and precipitation thus can contribute significantly to the removal of Asian dust storm particles from the atmosphere (Ma *et al.*, 2004b; Ma *et al.*, 2004c).

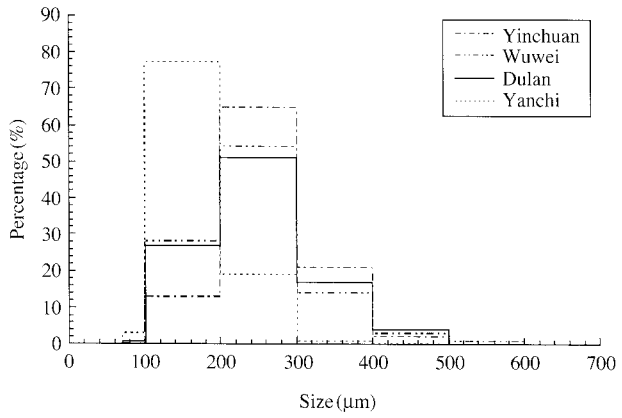

Fig. 2. Relative size distribution of original sands collected at four desert areas in China.

3.2 Chemical Properties

3.2.1 Bulk Desert Sands

Fig. 3 displays PIXE spectra of both insoluble (a) and soluble fraction (b) of original bulk sands collected in four different desert areas. In like with general expectation, soil originated components (such as Si, K, Ca, and Fe) are resolved as the remarkably high counts with no relevance to water solubility. The minor trace elements (like Cr, Cu, Zn, and Sr) are also in compliance with each channel number as small peaks in insoluble fraction of dust sands. Several elements in insoluble portion, especially Ca, have a relatively severe site-to-site variation with the maximum level in the sands of Dulan site. Elsewhere, in comparison to insoluble portion, albeit negligible in peak size relative to the other elements, Cl is found at the spectrum of water soluble portion.

The mass concentration (ng g^{-1}) for multielement can be quantitatively calculated by channel range and the characteristic X-ray count of each element. In order to conduct quantitative elemental analysis, the

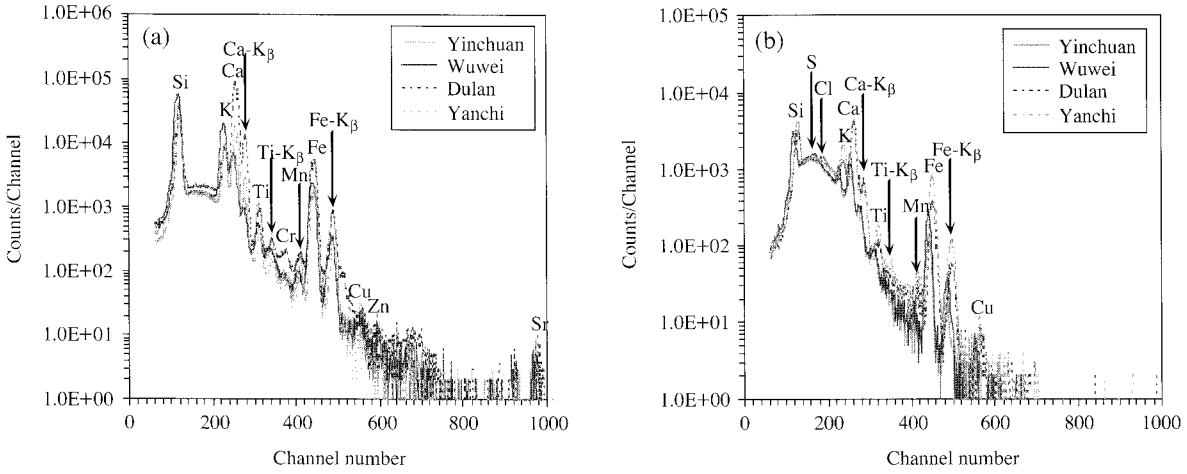

Fig. 3. PIXE spectra of insoluble (a) and soluble fraction (b) for original bulk sands collected in four different desert areas.

Table 1. The concentration ratios of Z/Si for four kinds of desert sands as a function of water solubility.

	Insoluble fraction				Soluble fraction			
	Yinchuan	Wuwei	Dulan	Yanchi	Yinchuan	Wuwei	Dulan	Yanchi
Si	1.0000	1.0000	1.0000	1.0000	1.0000	1.0000	1.0000	1.0000
S	N.D.[a]	0.0003	N.D.	N.D.	N.D.	N.D.	0.0282	N.D.
Cl	0.0008	0.0017	0.0036	0.0027	0.0386	0.0281	0.0404	N.D.
K	0.0530	0.0878	0.0761	0.1009	0.2231	0.1569	0.1818	0.1693
Ca	0.0473	0.0239	0.7011	0.2116	0.5063	0.3132	0.9620	0.3488
Ti	0.0035	N.D.	N.D.	N.D.	N.D.	N.D.	N.D.	N.D.
V	0.0042	0.0032	0.0076	0.0044	0.0000	0.0060	0.0107	0.0105
Cr	0.0015	0.0010	0.0056	0.0024	0.0077	0.0037	0.0098	0.0064
Mn	0.0046	0.0019	0.0072	0.0050	0.0100	0.0085	0.0176	0.0174
Fe	0.1666	0.0506	0.2077	0.0988	0.3682	0.3208	0.4007	0.4345
Cu	0.0018	0.0008	0.0022	0.0008	N.D.	N.D.	0.0063	0.0066
Zn	0.0011	0.0004	0.0017	0.0008	N.D.	N.D.	0.0036	0.0021
Sr	0.0014	0.0012	0.0027	0.0012	N.D.	N.D.	0.0081	0.0030
Pb	0.0003	0.0002	0.0008	0.0004	0.0059	0.0023	0.0025	0.0008

[a]Non-Detected.

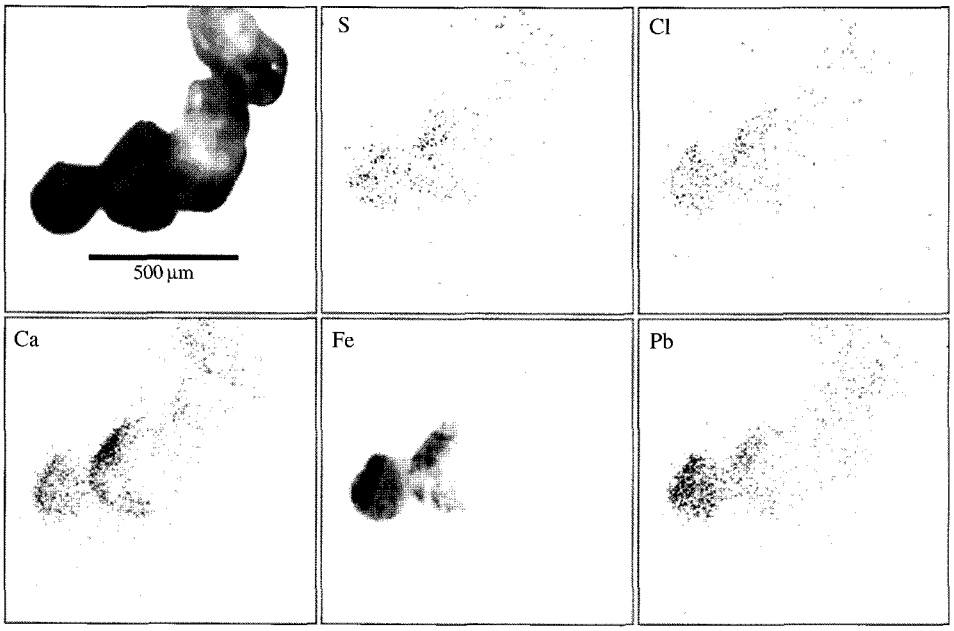

Fig. 4. The reconstructed XRF elemental maps corresponding to individual sands collected in at Yinchuan desert area.

masses of deposited sand powders onto polycarbonate substrate film have to be precisely measured. However, due to the small amount of pulverized sands homogenously mounted onto polycarbonate substrate film, it is not possible to conduct mass measurement. Hence, the concentration ratios of Z/Si are listed for soluble and insoluble fractions of the four kinds of desert sand in Table 1. Here, the concentration ratios of Z/Si were calculated by the initial result ($\mu g\ cm^{-2}$) of PIXE analysis. As might be expected, there is a tendency towards higher Z/Si ratios for soil derived elements such as : Si > Fe > K > Ca at Yinchuan, Si > K > Fe > Ca at Wuwei, Si > Ca > Fe > K at Dulan, and Si > Ca > K > Fe at Yanchi. Unfortunately, Al concentration cannot be reliably determined by our PIXE system. Although it has negligible ratio, S was detected in insoluble fraction of Wuwei sample with 0.0003 S/Si ratio and soluble fraction of Dulan sample with 0.0282 S/Si ratio. In addition, Cl was contained in every desert sand with the exception of the insoluble portion of Yanchi area. As reported by Mason (1966), some crustal rocks (such as shale and limestone) contain S and Cl. Therefore one should give attention to data interpretation about the aging processes of dust particles with sea-salts and man-made S. The relative elemental ratios summarized in Table 1 can be a means

to assess the transformation of dust particles during long-range transport and other aging processes.

3.2.2 Individual Desert Sands

An example of XRF elemental maps and microscopically imaged desert sands (top left) collected at Yinchuan desert area in China are presented in Fig. 4. It was possible to draw the distribution of components in and/or on desert sands. From XRF elemental maps, it can be visually confirmed that S, Cl, and Pb were present overall sand surface as the minor components. In contrast, Fe distribution is partially concentrated on sand surface. However, the elemental distribution on sand surface can be influenced by the degrees of an angle between Si(Li) detector recording the fluorescence X-rays and sample holder.

Fig. 5 shows the XRF spectra for four different points on a desert-sand in Fig. 4. These XRF spectra can be drawn by counting XRF counts of each element during the point analysis. The XRF spectra for four points on a sand show that point numbers 1, 3, and 4 are Fe and S-rich, while point number 2 has enrichment for only Fe. It thus suggests that the chemical property of desert sands shows the point-to-point variation. The summary of elemental mass concentration ($\mu g\ cm^{-2}$), calculated by XRF microprobe analysis for individual sands collected in at each desert area, is tabulated in Table 2. The elemental mass concentration for multielement can be quantitatively calculated by X-ray energy and count of each element with very low level sensitivity.

The result of point analysis by XRF microprobe with around 4 μm beam size shows the fluctuate variation of elemental mass concentration according to point. This dissimilar mass concentration depending on sand position indicates that the composition of individual desert sands is not homogeneous. The chemically inhomogeneous sands may be able to be chem-

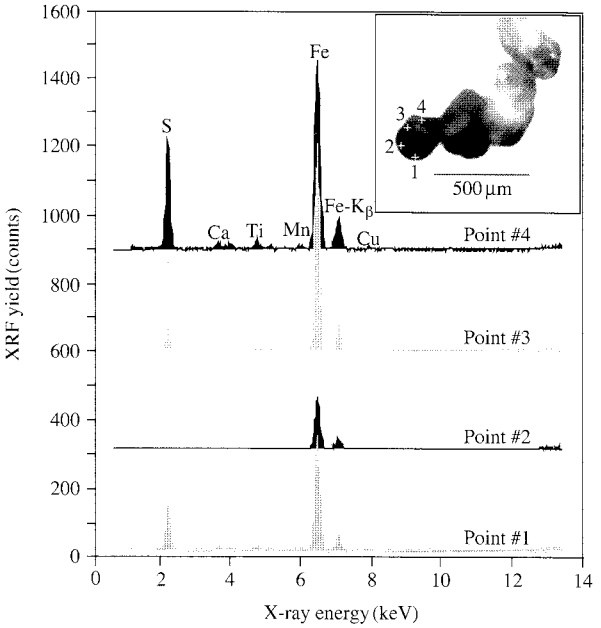

Fig. 5. The XRF spectra for four points on a single sand collected in at Yinchuan desert area.

Table 2. The summary of elemental mass concentration ($\mu g\ cm^{-2}$) calculated XRF microprobe analysis for individual sands collected in at each desert area.

	Yinchuan				Wuwei				Dulan				Yanchi			
	N[a]	Range	Average	Z/Si[b]	N	Range	Average	Z/Si	N	Range	Average	Z/Si	N	Range	Average	Z/Si
Al	33	1-411	44.3	0.229	8	0.14-102	42.8	0.115	18	35-1418	287	0.510	5	0.1-49	26	0.206
Si	33	7-871	193.7	1.000	8	3-1879	370.6	1.000	18	47-2767	563	1.000	5	0.117-311	128	1.000
P	33	1-55	13.4	0.069	8	0.169-57	19.3	0.052	18	18-202	76	0.134	5	0.019-12	6	0.048
S	31	0.14-28	6.7	0.035	7	0.127-24	7.8	0.021	18	19-171	63	0.111	5	0.031-5	2	0.018
Cl	33	0.08-23	4.8	0.025	8	0.015-17	4.9	0.013	18	41-298	99	0.175	5	0.025-6	3	0.020
K	33	0.14-682	40.2	0.207	8	0.141-22	8.6	0.023	18	10-2370	264	0.469	5	0.007-94	26	0.206
Ca	34	0.04-87	10.7	0.055	8	0.026-20	7.7	0.021	18	6-1893	428	0.760	5	0.017-34	12	0.096
Sc	33	0.04-10	2.0	0.010	8	0.001-6	1.8	0.005	18	3-164	41	0.072	5	0.002-5	3	0.020
Ti	34	0.06-170	18.9	0.097	8	0.012-20	5.9	0.016	18	2-242	36	0.064	5	0.011-45	15	0.120
V	32	0.08-32	5.3	0.027	8	0.003-10	2.7	0.007	18	1-33	8	0.014	5	0.002-7	4	0.028
Cr	34	0.02-9	1.9	0.010	8	0.006-7	1.8	0.005	18	2-26	5	0.009	5	0.014-6	3	0.021
Mn	33	0.06-36	5.6	0.029	8	0.006-9	2.8	0.007	18	1-57	8	0.014	5	0.006-14	7	0.051
Fe	34	0.24-182	55.6	0.287	8	0.162-62	25.2	0.068	18	4-268	101	0.179	5	0.026-118	58	0.456
Co	34	0.02-88	17.2	0.089	8	0.007-82	20.5	0.055	18	0.2-192	21	0.037	5	0.003-10	5	0.041
Ni	33	0.01-3	0.4	0.002	8	0.0005-5	1.1	0.003	18	1-8	2	0.003	5	0.003-1	0.3	0.003
Cu	34	0.004-2	0.3	0.002	8	0.002-7	1.7	0.005	18	0.4-3	1	0.001	5	0.004-1	0.3	0.003
Zn	33	0.004-2	0.5	0.003	8	0.0004-5	1.3	0.003	18	0.3-6	1	0.002	5	0.001-1	0.3	0.003

[a]Number of point analysis.
[b]Ratio of element to Si.

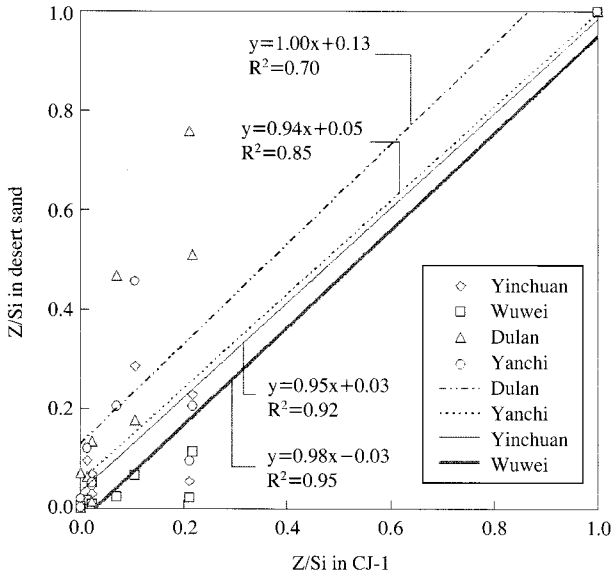

Fig. 6. Relationship between Z/Si in four types of local desert sands and Z/Si in the CJ-1.

ically homogeneous fine sand pieces via aeolian processes and then they blown off as the dust particles. Since the number of point analysis is not enough, the chemical property of individual desert sands can be comparable to that of bulk sands. However, the mass concentration has still enrichment for crustal elements like Al, Si, K, Ca, and Fe. They were exhibited a predominant occurrence in point analysis of individual sands.

Though it can not fully estimate the property of whole desert sand since a part of desert sand was irradiated by XRF, the elemental compositions of individual sands detected in the present study are comparable to those of bulkily analyzed reference desert sands. Fig. 6 shows the relationship between Z/Si in four-kind local desert sands and Z/Si in the CJ-1. Here, the elemental mass concentrations determined by XRF analyses for the individual sands of four-kind local desert were used. The elemental mass concentration of CJ-1, which is the stand desert sample of China loess, was provided by the Sino-Japan Friendship Centre for Environmental Protection (SJC). The coefficients of determination (R^2) of the ratio of each element to Si (Z/Si) between the individual sands collected from four local deserts and the bulk reference sands are varied from 0.70 to 0.95 (Fig. 6). Though some kinds of element are scattered from a one-to-one line, this result suggests that there is a relatively good accord between the individually estimated sand in this study and the bulk stand sand sample.

4. CONCLUSION

As the source of Asian dust particles, the sands at four different desert areas were to be the target of bulk and single analyses by means of PIXE and SR-XRF analyses, respectively. The physical properties of desert sands like morphology, color, and size were basically determined. Also the chemical characteristics of bulk sands of each desert were specified as the relative elemental ratio. The XRF elemental maps and spectra for a point on individual sands allow us to understand the nature of individual sands. Consequently, the physicochemical properties of desert sands obtained from this study can be helpful to understand what kinds of man-made pollutants and sea-salts are incorporated into natural Asian dust particles.

ACKNOWLEDGEMENTS

This study was supported in part by funds from the Grant-in-Aid for Scientific Research on Priority Areas under Grant No. 14048212 and 14048213 from the Ministry of Education, Culture, Sports, Science and Technology (MEXT), Japan. The synchrotron radiation experiments were performed at the SPring-8 with approval of the Japan Synchrotron Radiation Research Institute (JASRI) (Proposal No. 2002B0395 -NOS-np, 2002A4029-LM-np). The authors gratefully acknowledge Professor S. Hayakawa at Graduate School of Engineering, Hiroshima University for his analytical support.

REFERENCES

Bates R.L. and J.A. Jackson (eds.) (1987) Glossary of Geology. American Geological Institute, Alexandria, VA, p. 788.

Braaten D.A. and T.A. Cahill (1986) Size and composition Asian dust transported to Hawaii. Atmos. Environ., 20, 1105-1109.

China Development Brief, http://www.chinadevelopment brief.com.

Darzi M.D. and W. Winchester (1982) Aerosol characteristics at Mauna Loa observatory, Hawaii, after east Asia dust storm episodes. J. Geophys. Res., 87, 1251-1258.

Desboeufs K.V., R. Losno, and J.L. Colin (2001) Factors influencing aerosol solubility during cloud processes. Atmos. Environ., 35, 3529-3537.

Duce R.A., C.K. Unni, B.J. Ray, J.M. Prospere, and J.T. Merrill (1980) Long-range atmospheric transport of soil dust from Asia to the tropical north Pacific: Tem-

poral variability. Science, 209, 1522-1524.
Hayakawa S. (2000) X-ray fluorescence method for trace analysis and imaging. J. Japanese Soc. for Synch. Rad. Res., 13, 313-318. (in Japanese)
Hayakawa S., N. Ikuta, M. Suzuki, M. Wakatsuki, and T. Hirokawa (2001) Generation of an X-ray microbeam for spectromicroscopy at SPring-8 BL39XU. J. of Synch. Rad., 8, 328-330.
Husar R.B., D.M. Tratt, B.A. Schichtel, S.R. Falke, F. Li, D. Jaffe, S. Gassó, T. Gill, N.S. Laulainen, F. Lu, M.C. Reheis, Y. Chun, D. Westphal, B.N. Holben, C. Gueymard, I. McKendry, N. Kuring, G.C. Feldman, C. McClain, R.J. Frouin, J. Merrill, D. DuBois, F. Vignola, T. Murayama, S. Nickovic, W.E. Wilson, K. Sassen, N. Sugimoto, and W.C. Malm (2001) The Asian Dust Events of April 1998. J. Geophys. Res. Atmos., 106(D16), 18317-18330.
Iwasaka Y., M. Yamamoto, R. Imasu, and A. Ono (1988) Transport of Asian dust (KOSA) particles: importance of weak KOSA events on the geochemical cycle of soil particles. Tellus, 40B, 494-503.
Lafon S., J.-J. Rajot, S.C. Alfaro, and A. Gaudichet (2004) Quantification of iron oxides in desert aerosol. Atmos. Environ., 38, 1211-1218.
Ma C.-J., S. Tohno, M. Kasahara, and S. Hayakawa (2004a) Properties of individual Asian dust storm particles collected at Kosan, Korea during ACE-Asia. Atmos. Environ., 38, 1133-1143.
Ma C.-J., S. Tohno, M. Kasahara, and S. Hayakawa (2004b) The nature of individual solid particles retained in size-resolved raindrops fallen in Asian dust storm event during ACE-Asia, Japan. Atmos. Environ., 38, 2951-2964.
Ma C.-J., S. Tohno, M. Kasahara, and S. Hayakawa (2004c) Determination of the chemical properties of residues retained in individual cloud droplets by XRF microprobe at SPring-8. Nuc. Inst. and Methods in Phys. Res., B 217, 657-665.
Mason B. (1966) Principles of Geochemistry, 3rd edn. Wiley, New York.
Nishikawa M., Q. Hao, and M. Morita (2000) Preparation and evaluation of certified reference materials for Asian mineral dust. Global Environ. Res., 4, 103-113.
Qian W., X. Tang, and L. Quan (2004) Regional characteristics of dust stroms in China. Atmos. Environ., 38, 4859-4907.
Sino-Japan Friendship Centre for Environmental Protection (SJC) http://www.china-epc.cn/ japan/index_e.htm
Song C.H. and G.R. Carmichael (1999) The aging process of naturally emitted aerosol (sea-salt and mineral aerosol) during long range transport. Atmos. Environ., 33, 2203-2218.
Song M., M. Lee, K.J. Moon, J.S. Han, K.R. Kim, and G. Lee (2006) Chemical characteristics of fine aerosols during ABC-EAREX2005. J of Korean Soc. for Atmos. Environ., 22, 604-613.
Zhang D. and Y. Iwasaka (1998) Morphology and chemical composition of individual dust particles collected over Wakasa bay, Japan. J. of Aero. Sci., 29, S217-S218.

(Received 10 May 2008, accepted 20 July 2008)